# Improvement of Etalon-fringe Immunity in Diode-laser Derivative Spectroscopy

Ryuji Koga*, Megumi Kosaka*, Hiroya Sano*

## Synopsis

In a sensitive spectrometry with lead-salt diode lasers, etalon-fringe phenomena often intervene in the measured absorption spectrum. Derivative methods are employed for the purpose of high resolution where the pertaining wavelength is modulated. This paper presents results of mathematical examination on a possible improvement of immunity from the etalon-fringes by choosing the profile of the wavelength modulation.

## 1. Introduction

With the appearance of lead-salt diode lasers, absorption spectra in mid-infrared region have become to be measured finer than with grating monochromators. The lead-salt diode lasers are characterized by their quick tunability in addition to high brightness, coherence and spectral purity (1-3). The response of the frequency modulation extends up to about 16 kHz (4).

A traditional method of differential spectrometer is equipped with a vibrating slit, which modulates the wavelengh peridically. The electrical output signal is then processed by a phase-sensitive detector, and the extracted first or second harmonics of the slit frequency corresponds to the derivative of the absorption spectrum of the media in question. This method has a power to discern a weak but

---

* Department of Electronics.

sharp absorption line from an underlying broad spectrum (5-10).
Replacement of the spectrometer with a tunable diode results in very
high resolution and sensitivity.  Its application extends from a high
resolution spectroscopy to industrial instrumentations for field uses
(11-14).

According to the progress of the performance of the diode-laser
absorption spectrometry, a phenonena of etalon-fringe has often
limited its accuracy.  This arises from the excellent coherence of
the laser light.  If there is a couple of partially reflecting
surfaces across the light beam, an optical cavity, though its $Q$ is
very low, is formed and a periodic spectrum with very fine pitch is
superinposed on the measured absorption spectra.  This undesirable
spectrum is hardly rejected with a statistical data processing such
as accumulation of data nor a coaddition of the spectra.  A radical
elimination of the etalon-fringe should be made essentially through a
careful design and adjustment of optical system.  Aside this fact,
the authors have found that a suitable choice of the modulation
profile of the laser current leads to a good etalon-fringe
suppression.  Results of mathematical examinations are reported here.

This result has been brought through the research of the laser
gas analysis which has been carried out for years (15,16), but is
applicable to other field of spectrometries.


## 2. Description of Etalon Fringes

An etalon, in its original terminology, stands for an optical
instrument which is composed of two light-reflecting surface in
extremely good parallelism.  Its transmittance spectrum has a
periodic profile with period $1/d$ for the spacing of the surfaces, $d$.
The etalon, or Fabry-Perot interferometer, is used to attain an
extremely high resolution in a spectroscopy (17).

Also in an optical system of diode laser spectrometer to measure
an absorption spectrum in high resolution making the best of the high
spectral purity of the laser, a light beam necessarily transverse
across partially reflecting surfaces.  Some of the pairs may form an
optical configuration similar to the etalon though its $Q$ is very low
and the fringe is vague.

As it is commonly the case in an optical equipment,
antireflection coatings are put on surfaces of the optical elements,

and the optical configuration is so designed that the light beam should pass once through and any return beam should not couple with the main beam.  However, a coupling between the main and the refracted beam occurs inevitably, even if the above principle is achieved in a sense of geometrical optics.

An actual etalon-fringe consists of many modes, and the authors showed that an amplitude of each mode keeps still on the time-elapse but only its phase moves slowly (16).  From this fact, an accumulation of data or a coaddition of spectra are not effective. In many cases the etalon-fringe consists of components with periods finer than the dominamt Fourier transform component of the gas spectrum to be measured.  The method of smoothing (18) are generally employed to eliminate a noise whose spectral frequencies are higher than the inquired spectrum.  It is, however, ineffective for the etalon-fringes because its spectral profile is periodic and a very dense data sampling is required to avoide the aliasing.
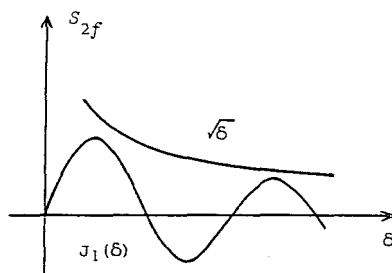


Fig.1 Response of 2*f* signal to the sinusoidal wavelength modulation
profile.  The envelope decreases slowly in the order of $\sqrt{\delta}$.

In Fig.1, a response of the second derivative signal is shown as a function of $\delta$, the ratio of the modulation width to the period of the etalon-fringe in case of a sinusoidal modulation profile.  The distribution is Bessel function of the first order and the envelope of the amplitude decreases in the order of $\sqrt{\delta}$ as $\delta$ tends to the infinitive.  Thus an etalon-fringe with high spectral frequency affects on the data and the problem of aliasing cannot be avoided even with a fine sampling pitch.

Thus etalon-fringes cannot be suppressed by a data processing and it must be suppressed before the analog to digital conversion.

## 3. Analysis of Derivative Spectrometry in $D$-space

### 3.1  Formulation of the Derivative Spectrometry

Let the transmittance spectrum of the material under inspection be $\exp(-\tau(\nu))$ for the monochromatic light of wavenumber $\nu$. In the derivative spectrometry, the $\nu$ is modulated as

$$\nu = \nu_0 - \Delta \cdot \eta(\vartheta), \tag{1}$$

where $\nu_0$ is the center wavenumber, $\Delta$, the amplitude and $\eta(\vartheta)$, the periodic modulation profile under the restrictions,

$$\eta(\vartheta+\pi) = -\eta(\vartheta), \tag{2}$$

$$\eta(-\vartheta) = -\eta(\vartheta), \tag{3}$$

and

$$-1 \leqq \eta(\vartheta) \leqq 1. \tag{4}$$

The variable $\vartheta$ is incorporated instead of the time. Due to the restriction of Eqs.(2) and (3), $\eta(\vartheta)$ is fully described by $\eta(\vartheta)$, $-\frac{\pi}{2} \leqq \vartheta \leqq \frac{\pi}{2}$, though the period is $2\pi$.

A schematic diagram of the derivative spectrometry is described in Fig.2. The output, $S_{2f}$, called as the $2f$ signal, is written by

$$S_{2f} \fallingdotseq \frac{1}{\pi} \int_{-\pi}^{\pi} \tau\{\nu-\Delta\cdot\eta(\vartheta)\}\cos 2\vartheta\, d\vartheta . \tag{5}$$

This expression is rewritten as

$$S_{2f} = \frac{2}{\pi} \int_{-1}^{1} \tau(\nu_0-\Delta\cdot\eta)\,\tilde{w}(\eta)\, d\eta, \tag{6}$$

where $\tilde{w}(\eta)$ is a weight distribution defined by

$$\tilde{w}(\eta) = \frac{d\vartheta}{d\eta} \cos 2\vartheta . \tag{7}$$

An inverse function $\vartheta(\eta)$ is employed here. The expression of Eq.(6) is no more than an convolution between $\tau(\nu)$ and a weight distribution $w(\eta)$ of
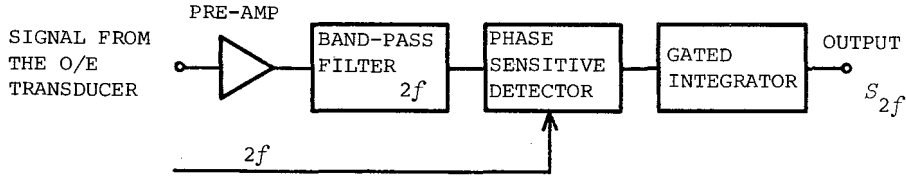
Fig.2  Blockdiagram of a phase-sensitive detector which yields $2f$
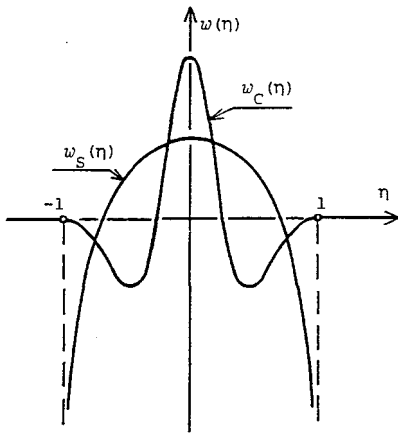signal from the opto-electric transducer output.



Fig.3  Weight distributions $w_S(\eta)$ and
$w_C(\eta)$.  The $w_S(\eta)$ for the sinusoidal
frequency-modulation profile has singu-
larity at $\eta=\pm 1$, whereas $w_C$ for the
inverse integrated raised cosine(IIRC)
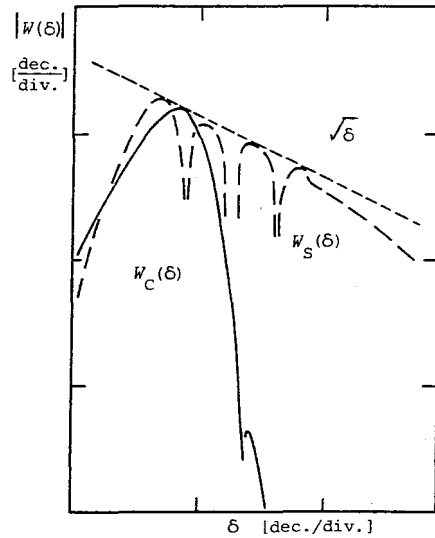profile is smooth everywhere.



Fig.4 Spectra of $W_S$ and $W_C$.  The enve-
lope of $W_S$ decreases slowly with $-1/2$
inclination in the figure, whereas $W_C$
has very steep decrease in the right
side of the transmission band.

$$w(\nu) = \begin{cases} 0 & |\nu| > \Delta \\ w(\nu/\Delta) & |\nu| \leqq \Delta \end{cases} . \tag{8}$$

Fourier transforms of these functions of $\nu$, the wavenumber, are the functions of $D$ that has a dimensions of length. The Fourier transform of the $S_{2f}$ is written as

$$\mathcal{F}[S_{2f}] = T(D) \cdot W(D) \tag{9}$$

where $T(D)$ and $W(D)$ are Fourier transforms of $\tau(\nu)$ and $w(\nu)$, respectively.

A sinusoidal profile is generally adopted as the modulation profile in a derivative spectrometry even when a laser-diode is employed as a quickly tunable light source. In this case, $w(\eta)$ becomes

$$w(\eta) = w_S(\eta) \equiv \frac{1-2\eta^2}{\sqrt{1-\eta^2}} , \quad |\eta| \leqq 1, \tag{10}$$

whose profile is drawn in Fig.3, and its Fourier transform in Fig.4 in terms of the normalized spectral frequency $\delta$. Since $w_S(\eta)$ has a very sharp spike at $\eta = \pm 1$, its Fourier transform has slow decay as $\delta$ tends to infinitive. The envelope has a slope of -1/2 in the figure, which has been predicted in Section 2. This leads to an undesired response to an etalon-fringe of a very fine pitch.

In order to reduce the band-width of $W(D)$ as narrow as possible, it is desirable that $w(\eta)$ has a factor of $(1+\cos\pi\eta)$. This fact is well known in the field of the pulse communication technology (19). Let incorporate this factor in Eq.(7) through the $d\vartheta/d\eta$. Then an ordinary differential equation

$$\frac{d\vartheta_c}{d\eta} = \frac{\pi}{2}(1+\cos\pi\eta) \tag{11}$$

with the initial condition

$$\vartheta_c(0) = 0 \tag{12}$$

is obtained. This leads to a modulation profile of an inverse integral raised cosine(IIRC), viz,

$$\vartheta(\eta) = \frac{1}{2}(\pi\eta + \sin\pi\eta) \tag{13}$$

and the corresponding weight distribution

$$w(\eta) = w_C(\eta) \equiv \pi \cdot \cos(\pi\eta + \sin\pi\eta) \cdot (1+\cos\pi\eta) . \tag{14}$$

The profile $w_C(\eta)$ and its Fourier transform are shown in Figs.3 and 4, and the modulation profile in Fig.5.
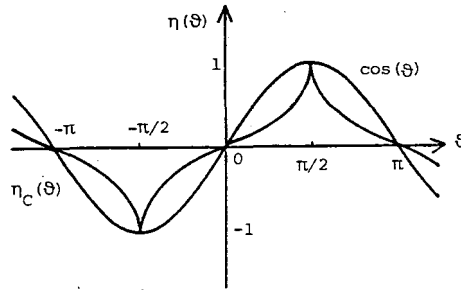


Fig.5 Profiles of laser frequency modulation over a fundamental period. The sinusoidal profile $\eta_S(\theta)$ and the inverse integrated raised cosine profile $\eta_C(\theta)$ are shown. The variable $\theta$ stand for the elapse of time.

As has been expected, $W_C(\delta)$ rolls off very rapidly as $\delta$ increases. This spectral features give rise to an immunity to an etalon-fringes of a fine pitch. The IIRC modulation profile is, however, impossible to be realized with a real electronic circuit since the profile has spikes at $\eta=\pm1$, requiring the infinite bandwidth. The reason why $W_C(\delta)$ occupies the narrowest bandwidth is just that the modulating profile has the infinite inclination at $\eta=\pm1$ or at $\vartheta=\pm\frac{\pi}{2}$ which leads the smooth transition of $w(\eta)$ at $\eta=\pm1$.

In order to approximate the IIRC profile within the limit of finite bandwidth of an electronic circuits, the exponential profile comes out as an candidate. The profile is written as

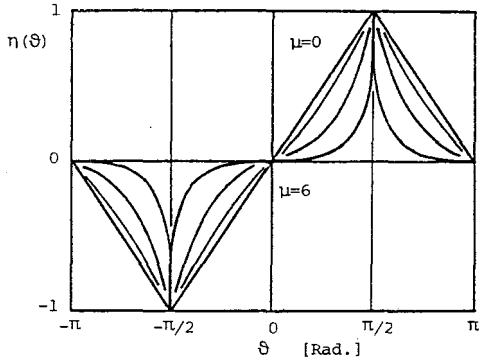$$\eta(\vartheta) = \eta_H(\vartheta) \equiv \frac{\sinh(\frac{2}{\pi}\mu\vartheta)}{\sinh\mu} , \tag{15}$$
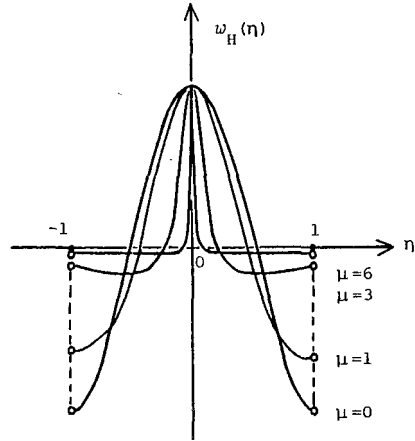
Fig.6 Profiles of the exponential law for μ=0,1,3 and 6.



Fig.7 Weight distributions for the exponential modulation profiles. These have discontinuities at η=±1.
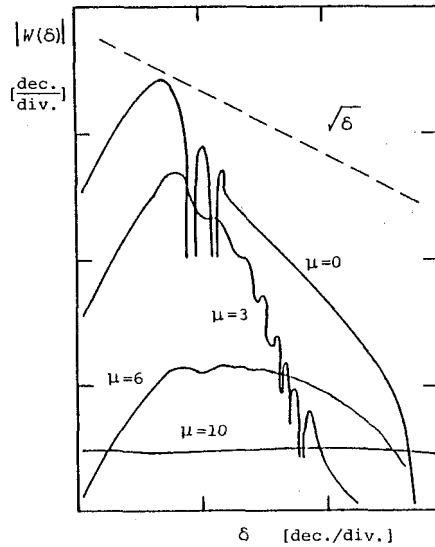


Fig.8 Spectra of $W_H$ for various μ's. Steeper roll-off is obtained for μ below 6 than $\sqrt{\delta}$ line which is characteristic to the $W_S$. Fine ripples are due to the finite temporal domain in FFT calculation.

which leads to the weight distribution of

$$w_H(\eta) = \cos\{2\vartheta_H(\eta)\} \frac{d\vartheta_H}{d\eta} . \tag{16}$$

The inverse modulation profile $\vartheta(\eta)$ is described as

$$\vartheta_H(\eta) = \frac{\pi}{2} \ln(\eta \sinh\mu + \sqrt{\eta^2 \sinh^2\mu + 1}) \tag{17}$$

and

$$\frac{d\vartheta_H}{d\eta} = \frac{\mu}{2\pi} \sqrt{\eta^2 \sinh^2\mu + 1} \tag{18}$$

having the parameter $\mu$. For $\mu=0$, the profile $\vartheta_H(\eta)$ coincide with the triangular shape. For various values of $\mu$, the modulation profiles are shown in Fig.6, the weight distribution in Fig.7, and their Fourier transform $W_H$ in Fig.8 along with the line of $-1/2$ inclination which corresponds to $W_S$. Considerable improvement is found in the suppressed response in the higher region of $\delta$ which gives an etalon-fringe immunity. From these traces, the parameter should be taken to be $\mu=3$ for the steepest inclination at the right side of the transmission band. This profile can be obtained with an operational amplifier circuit employing semiconductor diodes as nonlinear elements.


## 4. Concluding Remarks

A derivative spectrometry with a tunable diode laser is susceptible to an etalon-fringe with fine pitch if the frequency modulation profile is sinusoidal. It is mathematically shown that the exponential profile with $\mu \dot{=} 3$ which can be realized electronically will give rise to a higher immunity to the etalon-fringe. Experiments are under preparation.

## References

(1) E. D. Hinkeley, A. R. Calawa, P. L. Kelley and S. A. Clough: J. Appl. Phys., 43(1972)3222.

(2) J. R. Aronson, P. C. von Tuna and J. F. Butler: Appl. Opt., 14(1975)1120.

(3) M. Wahlen, R. S. Eng and K. W. Nill: Appl. Opt., 16(1977)2355.

(4) S. Nagase, R. Koga, M. Kosaka and H. Sano: Trans. IECE, 63-C(1980)317.

(5) A. Perregaux and G. Ascarelli: Appl. Opt., 7(1968)2031.

(6) D. T. Williams and R. N. Hager, Jr.: Appl. Opt. 9(1970)1597.

(7) R. Zucca and Y. R. Shen: Appl. OPt., 12(1973)1293.

(8) R. N. Hager, Jr. and R. C. Anderson: J. Opt. Soc. Am., 60 (1970)1444.

(9) F. Grum, D. Paine and L. Zoeller: Appl. Opt., 11(1972)93.

(10) T. C. O'Haver and G. L. Green: Anal. Chem., 48(1976)312.

(11) R. T. Ku, E. D. Hinkley and J. O. Sample: Appl. Opt., 14(1975)854.

(12) E. D. Hinkley, R. T. Ku, W. Nill and J. F. Butler: Appl. Opt., 15(1976)1653.

(13) J. Reid, J. Shewchun, B. K. Garside and E. A. Ballik: Appl. Opt., 17(1978)300.

(14) J. Reid, B. K. Garside, J. Shewchun, M. El-Sherbiny and E. A. Ballik: Appl. Opt., 17(1978)1806.

(15) R. Koga, S. Nagase, M. Kosaka and H. Sano: Memoirs School Eng., Okayama Univ., 15-1(1980)47.

(16) R. Koga, S. Nagase, M. Kosaka and H. Sano: Memoirs School Eng., Okayama Univ., 15-2(1981)79.

(17) F. A. Jenkins and H. E. White: "Fundamentals of Optics" McGraw-Hill(1976), Chap.14.

(18) A. Savitzky and M. J. E. Golay: Anal. Chem., 36(1964)1627.

(19) R. W. Luckey and E. J. Weldon: "Principles of data communication" McGraw-Hill(1968).